

Original Research

Finite element analysis of the effect of sagittal angle on ankle joint stability in posterior malleolus fracture: A cohort study

Ming Guan^a, Jing Zhao^c, Yong Kuang^d, Guang Li^{b,**}, Jun Tan^{a,*}^a Department of Spine surgery, Shanghai East Hospital, Tongji University School of Medicine, Shanghai, 200120, China^b Department of Traumatology, Shanghai East Hospital, Tongji University School of Medicine, Shanghai, 200120, China^c Department of Nursing, Shanghai East Hospital, Tongji University School of Medicine, Shanghai, 200120, China^d Department of Orthopedics, Shanghai Artemed Hospital, Shanghai, 200131, China

ARTICLE INFO

Keywords:

Posterior malleolus fracture
Finite element analysis
Sagittal angle
Ankle stability

ABSTRACT

Objective: Aim of this study was to establish three-dimensional finite element model of the posterolateral-oblique type of posterior malleolus fracture with different sagittal angle and to explore the effect of sagittal angle on ankle joint stability.

Methods: CT data of ankle were collected from a normal male volunteer. Established finite element model of the normal ankle and verified its reliability. Five posterior malleolus fracture models with different sagittal angles were established. Finite element analysis (FEA) was carried out to simulate the conditions of vertical loading in neutral position with a total weight of 600 N. Recorded the data and did statistical analyses.

Results: (1) The contact area was 483.55 mm² and the maximum contact stress was 3.793 MPa in the model of the normal ankle joint. (2) There was a positive correlation between the sagittal angle (SA) and the contact area (CA) ($r = 0.925, P < 0.05$). Regression equation was $CA = 316.755 + 1.749 * SA$. The correlation between the sagittal angle and the maximum contact stress (MCS) was negative ($r = -0.988, P < 0.01$). Regression equation was $MCS = 5.214 - 0.018 * SA$. There was a negative correlation between the sagittal angle of fracture and relative displacement (RD) ($r = -0.950, P < 0.05$). Regression equation was $RD = 1.388 - 0.009 * SA$.

Conclusion: The greater the sagittal angle of fracture was, the more stable the ankle joint was. The sagittal angle of fracture could be used as a relative index to reflect ankle stability for posterior malleolus fracture.

1. Introduction

Ankle fractures are relatively common injuries with an incidence of 10% among all fractures [1]. Posterior malleolus fractures are 10%–44% of total ankle fractures [2,3]. Posterolateral-oblique posterior malleolus fractures are about 67% of all posterior malleolus fractures [4]. Many studies have focused on the effect of fracture size on ankle stability on the horizontal axis. Most of the researchers agreed with the recommendation that the posterior fragment involving greater than 25% of the articular surface would affect the stability of ankle joint [1,4,5]. In fact, the fracture fragments are three-dimensional structures and their performances on the neutral axis are different. Luo et al. measured the sagittal angle of posterior malleolus fracture, which could be regarded as an important index of relative height of fracture fragments in the three-dimensional structure, relative to the neutral axis and the major fracture line of the posterior fragment on the sagittal

reconstruction images with the use of CT [6]. Finite element analysis technology (FEA) is a modern computational method based on structural mechanics analysis. The result of FEA would be as close as possible to the real ontology [5]. The purpose of this study was to establish posterolateral-oblique posterior malleolus fracture models with different sagittal fracture angles and to analyze their effectiveness with FEA. The effect of the sagittal angle of fracture on ankle joint stability was discussed.

2. Materials and methods

2.1. Design

This research work was approved by the Medical Research Ethics Committee of our hospital and was performed in accordance with the Declaration of Helsinki. It was registered on ChiCTR too. This study was

* Corresponding author. No.150 Ji Mo Road, Pu Dong New District, Shanghai, 200120, China.

** Corresponding author. No.150 Ji Mo Road, Pu Dong New District, Shanghai, 200120, China.

E-mail addresses: 13681826275@139.com (G. Li), 13761092637@139.com (J. Tan).

<https://doi.org/10.1016/j.ijss.2019.08.022>

Received 20 May 2019; Received in revised form 30 July 2019; Accepted 12 August 2019

Available online 17 August 2019

1743-9191/ © 2019 IJS Publishing Group Ltd. Published by Elsevier Ltd. All rights reserved.

a cohort study. Finally, the work should be reported in line with the STROCSS criteria [7].

2.2. Materials

Data: A 25-year-old male volunteer, 170 cm in height and 60 kg in weight, had no history of foot trauma. Imaging examination excluded bone lesions such as foot tumors, deformities and fractures.

Equipment: Philips Brilliance 64-slice spiral CT (provided by East Hospital Affiliated to Tongji University).

Computer workstation: Intel (R) Core (TM) i7-6700HQ CPU @ 3.50 GHz, memory: 16.0G, Graphics card: Nvidia Quadro M1200 (4 GB).

Software: Medical Image Processing Modeling Software: Mimics Medical 21.0, 3-matic Medical 13.0(Materialise corp., Belgium), Mesh Generation and Finite Element Modeling Software: Hypermesh 2017(Altair corp., USA), Finite Element Analysis Software: Optistruct 2017(Altair corp., USA), Statistical analysis software:SPSS 23.0 (IBM corp., USA).

2.3. Methods

2.3.1. Data acquisition

Volumetric CT scan was performed on of the right ankle joint of the volunteer. The volunteer's right foot remained in neutral position, ranging from 1/3 of the middle and lower tibia and fibula to the whole foot during the CT scan. 408 right foot CT images with 512*512 pixels were obtained and the thickness of the images was 0.625 mm. The images were saved in Dicom format.

2.3.2. Establishment of finite element model of ankle joint

Mimics 21.0 software was used to reconstruct the right ankle CT images of the volunteer. STL geometric models including lower tibia and fibula, talus and calcaneus were obtained. Then 3-matic Medical 13.0 software was used to smooth, denoise, subdivide and repair the meshes of the imported geometric model. The geometric models of cartilage and ligament were built according to the anatomical relationship between the bones and ligaments (1 mm thickness on the surfaces of tibia, fibula and talus was set to the cortex of bone, and the inner part was cancellous bone. The thickness of cartilage was about 1.0 mm [5]. Ligaments included anterior tibiofibular ligament, posterior tibiofibular ligament, anterior talofibular ligament, posterior talofibular ligament, deltoid ligament, calcaneofibular ligament, etc.). The geometric model was imported into Hypermesh 2017. Meshing and material property distributions (Table 1) were carried out [8].Finally, the finite element model was obtained.

2.3.3. Validation of ankle joint model

Load Constraints, Contact Conditions and Friction Coefficient were added into Hypermesh 2017. Joint surface was defined as Coulomb friction contact and the friction coefficient was 0.01 [9]. The friction

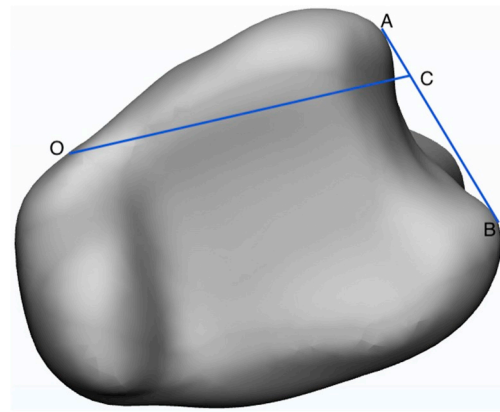


Fig. 1. Sketch map of horizontal fracture line.

coefficient of the fracture surface was 0.3 [5]. Ligaments were applied to the model as preload by reducing the length of ligaments by 2% with zero load [6]. When 600 N stress was loaded vertically in neutral position, the lower surface of calcaneus and the upper end of tibia were fixed and restrained, so that the calcaneus couldn't move relatively, while the tibia was kept moving vertically. Then the finite element analysis solutions were carried out by Optistruct 2017. The contact area, maximum contact stress and relative displacement of fractures were obtained.

2.3.4. Establishment of FEA fracture models with different sagittal angles

The finite element models of fracture were based on the finite element model of the normal ankle joint. Set X axis (lateral to medial of ankle joint), Y axis (toe to heel, XY plane parallel to plantar plane), Z axis (heel to knee joint upward). The horizontal projection of distal tibial articular surface was taken as the reference plane. The AB line of fibular notch projection on the plane was taken as the reference line. The 1/4 point of the AB line was taken as point C. The intersection point of the posterior ankle and medial ankle was the "O" point, and the OC line was connected as the horizontal fracture line(Fig. 1). The angle between the fracture line and the Z axis on the sagittal reconstruction images was defined as the sagittal angle of the posterior malleolus fracture [6](Fig. 2).The basic working plane rotated in the direction of XY plane while the line OC was unchanged. Five groups of fracture models with different angles were obtained finally when the sagittal angles were set to 3.3°, 18.3°, 33.3°, 48.3° and 63.3°(Fig. 3).

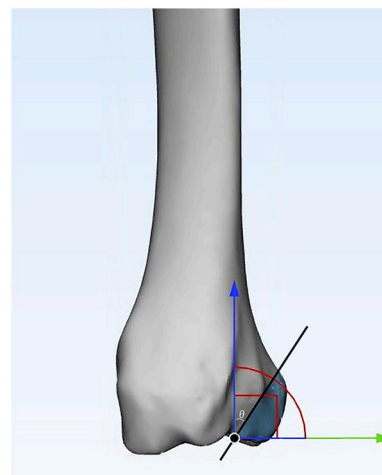


Fig. 2. Sketch map of sagittal angle.

Table 1
Material property settings.

	Density (g/cm ³)	Elastic modulus (MPa)	Poisson ratio
Compact bone	4.65exp-3	1.21exp4	0.30
Trabecular bone	1.81 exp-3	530.90	0.30
Articular cartilage	1.94 exp-3	0.83	0.49
Anterior talobular	1.94 exp-3	15.00	0.49
Posterior talobular	1.94 exp-3	15.00	0.49
Calcaneobular	1.94 exp-3	11.00	0.49
Anterior tibiobular	1.94 exp-3	16.55	0.49
Posterior tibiobular	1.94 exp-3	18.44	0.49
Deltoid	1.94 exp-3	7.00	0.49

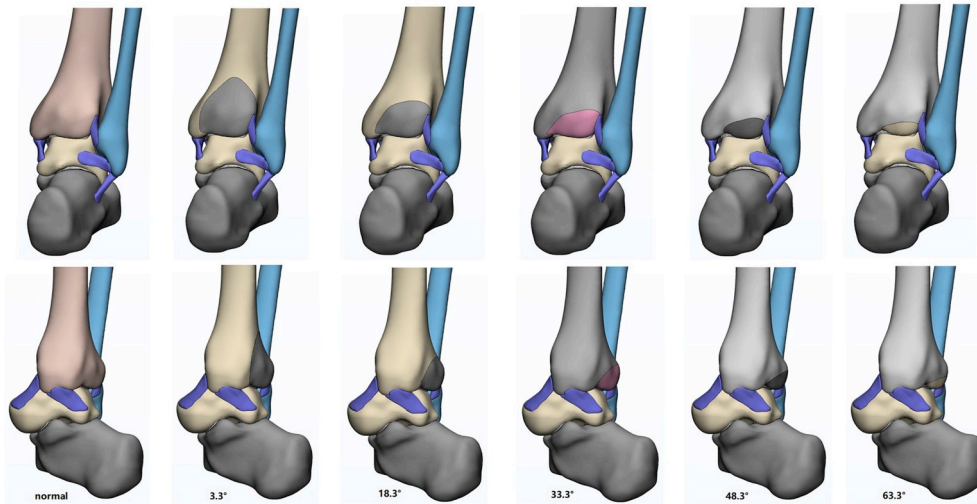


Fig. 3. Normal and five different sagittal angle fracture models.

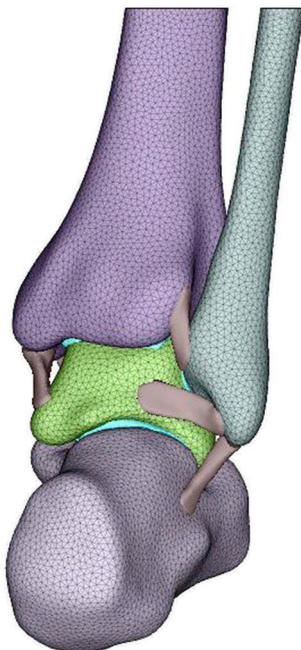


Fig. 4. Finite element model of normal ankle joint.

2.3.5. Calculation of finite element models with different sagittal angles

Five groups of fracture models were introduced into Hypermesh 2017 to do calculation of finite element according to the method 2.3.3. The contact area, maximum contact stress and relative displacement were obtained finally.

2.3.6. Statistical analysis

The data were processed by SPSS 23.0. The relationships between sagittal angle of fracture and articular contact area, maximum contact stress and relative displacement were correlation analyzed with Pearson correlation analysis. P value was considered significant if $p < 0.05$. If there was a linear correlation between them, the simple regression analysis would be carried out to get the regression equation.

3. Results

3.1. Establishment and verification of ankle joint finite element model

The finite element model with 441478 meshes was obtained (Fig. 4).

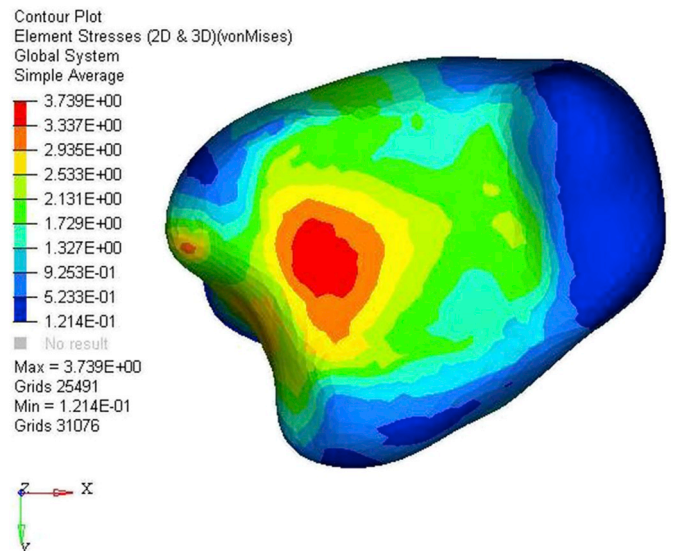


Fig. 5. Von-Mises stress distribution of normal ankle joint.

After 600 N stress was loaded vertically, the contact area of the joint surface was 483.55 mm^2 and the maximum contact stress was 3.793 MPa. The stress distribution is shown below (Fig. 5). Compared with other researchers' data [10,11], there was no significant difference (Table 2).

3.2. Finite element analysis of different sagittal angles of fractures

Five groups of fracture models were analyzed by finite element method, and the contact area, maximum contact stress and relative displacement of fracture were obtained. The results were in Table 3. The Von-Mise stress distributions were in Fig. 6.

3.3. Statistical analysis

3.3.1. The relationship between sagittal angle(SA) and contact area(CA)

The measured data were input into SPSS 23.0. The sagittal angle of fracture was taken as X axis and the contact area was taken as Y axis respectively. The scatter plot was created (Fig. 7). It was obvious that there was a linear relationship. Pearson linear correlation analysis was used to verify the results. The results were as follows: $r = 0.925$, $P < 0.05$. Therefore, the contact area of articular surface was

Table 2
Compared with other researchers' data.

	Anderson [10]		Hurschler [11]		This Study
	Tekscan	FEA	FEA	FEA	
Maximum contact stress(MPa)	3.69	3.74	4.4		3.793

Table 3
Results of FEA.

	3.3°	18.3°	33.3°	48.3°	63.3°
Contact Area(CA)(mm ²)	302.04	369.12	389.87	392.32	421.60
Maximum contact stress(MCS) (MPa)	5.095	4.882	4.687	4.368	3.969
Relative Displacement(RD) (mm)	1.448	1.135	1.034	0.944	0.859

positively correlated with the sagittal angle of fracture. Simple regression analysis was used to obtain the regression equation: CA = 316.755 + 1.749* SA.

3.3.2. The relationship between sagittal angle(SA) and maximum contact stress(MCS)

The measured data were input into SPSS 23.0. The sagittal angle of fracture was taken as X axis and the maximum contact stress was taken as Y axis respectively. The scatter plot was created (Fig. 8). It was obvious that there was a linear relationship. Pearson linear correlation analysis was used to verify the results. The results were as follows: r = -0.988, P < 0.01. So the maximum contact stress was negatively correlated with the sagittal angle of fracture. Simple regression analysis was used to obtain the regression equation: MCS = 5.214-0.018*SA.

3.3.3. The relationship between sagittal angle (SA) and relative displacement (RD)

The measured data were input into SPSS 23.0. The sagittal angle of

fracture was taken as X axis and the relative displacement was taken as Y axis respectively. The scatter plot was created (Fig. 9). It was obvious that there was a linear relationship. Pearson linear correlation analysis was used to verify the results. The results were as follows: r = -0.950, P < 0.05. Therefore, the relative displacement was negatively correlated with the sagittal angle of fracture. Then simple regression analysis was used to obtain the regression equation: RD = 1.388-0.009*SA.

4. Discussion

Current studies have shown that the posterior ankle can increase the contact area of the tibial-talus joint and reduce the unit area pressure of the tibial-talus joint [5]. Posterior ankle fracture may affect ankle stability and tibial-talus joint pressure. Any single osteotomy model can only provide limited damage mechanism [4]. In our study the results of contact area, the maximum contact stress and stress distribution were similar to other biomechanics and finite element results. It was proved that the model was reliable and effective. So the fracture model based on the model can be considered to be similar to the actual fracture situation.

It is generally believed that fractures involving more than 25% of the lateral phases [12] and fractures with displacement more than 1 mm [13] have surgical indications. In fact, the fracture fragments are three-dimensional structures, and their performances on the neutral axis are different. Luo et al. made the concept of sagittal angle of fracture through retrospective analysis of 650 patients' CT films with posterior ankle fracture. The angle was from 3.3° to 63.9° [6]. The sagittal angle is a good factor to evaluate the 3D size of fracture fragments. It can not only show the height of the fragment but also reflect the relationship between the height and the length of the fragment. In our study, the sagittal angles of five fracture groups were set to 3.3°, 18.3°, 33.3°, 48.3° and 63.3° what were approximately equal to the actual situations. In the results, when the sagittal angle increased, the contact area increased gradually and got close to the normal joint contact area, which was 483.55 mm². The maximum contact stress decreased

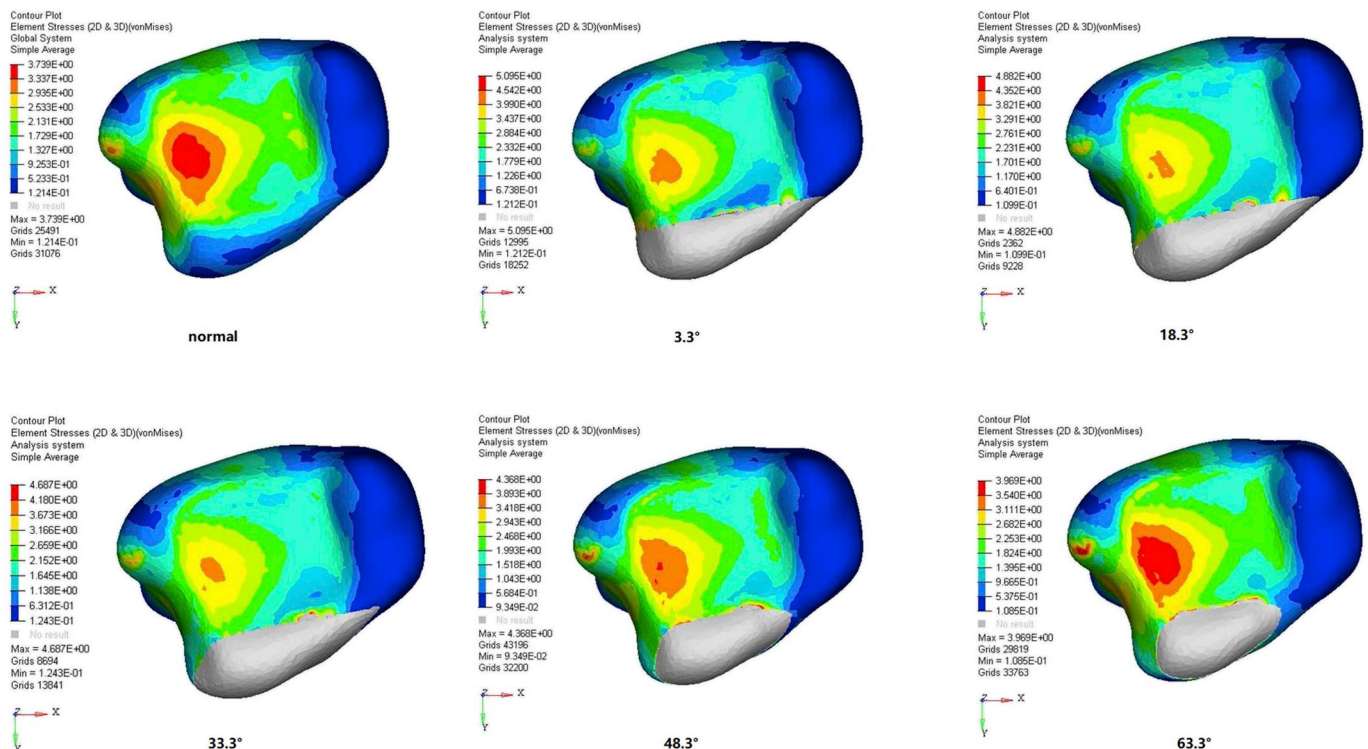


Fig. 6. Von-mise stress distributions in different models.

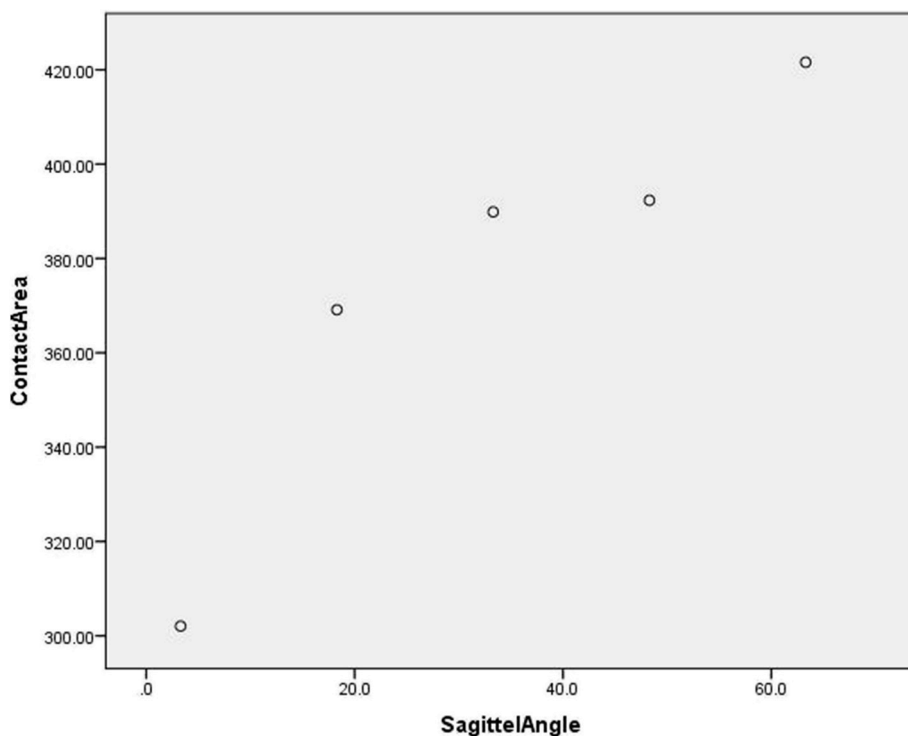


Fig. 7. The scatter plot of CA and SA.

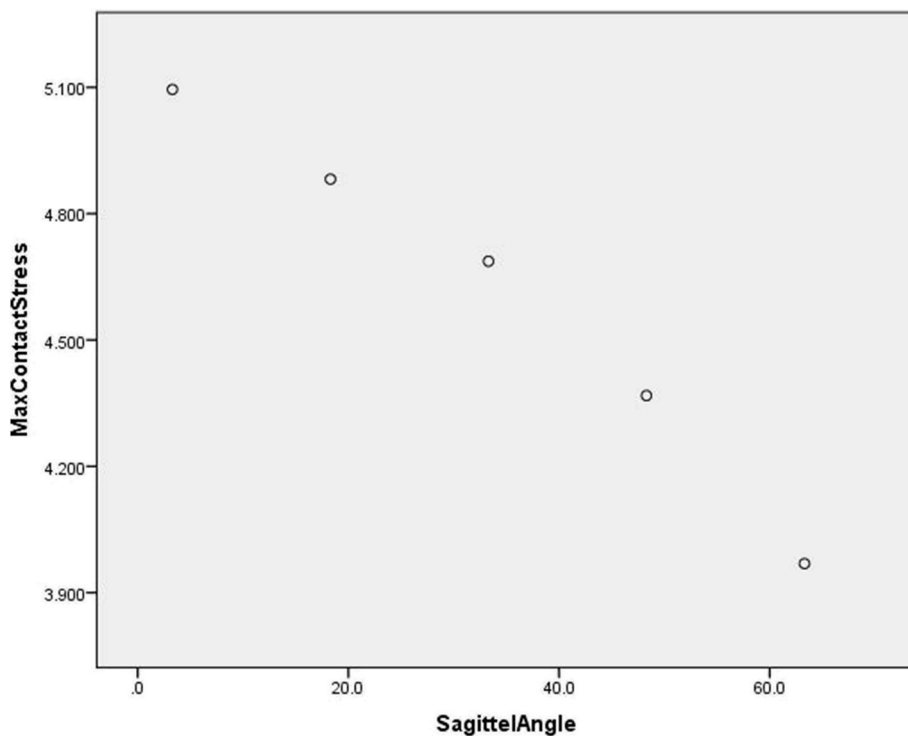


Fig. 8. The scatter plot of MCS and SA.

gradually from 5.095 MPa to 3.969 MPa that was close to the contact stress of the normal articular surface, which was 3.793 MPa. And the stress distribution turned be normal gradually. The relative displacement was negatively correlated with the sagittal angle. The regression equation was $RD = 1.388 - 0.009 \times SA$. From the equation, the sagittal angle can be obtained as 43.3° when the relative displacement was equal to 1 mm. It can be considered that when the sagittal angle of the

fracture was greater than 43.3° , the displacement distance of the fracture was less than 1 mm and there was no surgical indication in clinic. All of the above meant the stability of ankle joint increased too. These results may be attributed to the increase of the sagittal angle of fracture that led to the decrease of shear force between fractures, so the stability of fracture was higher.

There were still several limitations in this study. The homogeneous

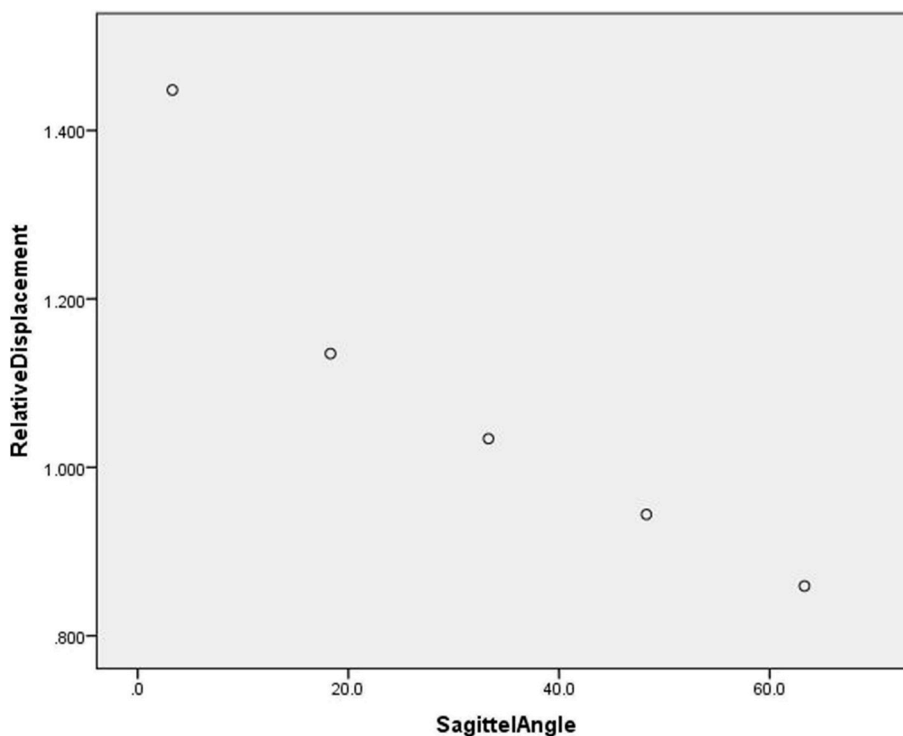


Fig. 9. The scatter plot of RD and SA.

and linearly elastic material properties were assigned to the bony and ligamentous structures to simplify the analysis. Many other bones and ligaments were not considered. All these limitations may result in a little differences between finite element analysis results and actual situations. But they have no influence on the value of the sagittal angle. Sagittal angle should be considered together with the area ratio of the fracture to the articular surface in further research.

5. Conclusion

The sagittal angle of fracture is an important factor affecting the stereoscopic structure of posterior malleolus fracture. It is significantly correlated with the maximum stress distribution on the articular surface, the contact area of the articular surface and the relative displacement of the fracture, so it obviously affects the stability of the ankle joint. So we can conclude that doctors should pay attention to the individual differences of patients with posterior malleolus fracture and consider the sagittal angle of the fracture as an index to fix the fracture.

Ethical Approval

Ethical Approval was given by Shanghai East Hospital, Tongji University School of Medicine, Shanghai, China.
The number is [2019] Pre-trial No. (016).

Sources of funding

None.

Research Registration Unique Identifying Number (UIN)

Chinese Clinical Trial Registration.
ChiCTR1900022958.
<http://www.chictr.org.cn/showprojen.aspx?proj=38549>.

Author contribution

Jun Tan: Conceptualization, Study design.
Ming Guan: Data analysis, Writing.
Jing Zhao: Data collections.
Yong Kuang: Supervision.
Guang Li: Methodology,

Conflicts of interest

None.

Guarantor

Jun Tan.
Guang Li.

Competing financial interests

The author(s) declare no competing financial interests.

Provenance and peer review

Not commissioned, externally peer-reviewed.

Data statement

The data is true and reliable without plagiarism.

CRediT authorship contribution statement

Ming Guan: Software, Writing - original draft. **Jing Zhao:** Formal analysis. **Yong Kuang:** Investigation, Validation. **Guang Li:** Data curation, Supervision. **Jun Tan:** Conceptualization, Project administration, Writing - review & editing.

Appendix A. Supplementary data

Supplementary data to this article can be found online at <https://doi.org/10.1016/j.ijvs.2019.08.022>.

References

- [1] S. Tenenbaum, N. Shazar, N. Bruck, J. Bariteau, Posterior malleolus fractures, *Orthop. Clin. N. Am.* 48 (1) (2017) 81.
- [2] K.J. Koval, J. Lurie, W. Zhou, et al., Ankle fractures in the elderly: what you get depends on where you live and who you see, *J. Orthop. Trauma* 19 (9) (2005) 635–639.
- [3] M.L. Prasarn, D.G. Lorich, Posterior malleolus fractures in athletes, *Oper. Tech. Sport. Med.* 25 (2) (2017) 82–86.
- [4] N. Haraguchi, H. Haruyama, H. Toga, F. Kato, Pathoanatomy of posterior malleolar fractures of the ankle, *J. Bone Joint Surg. Am.* Vol. 88 (5) (2006) 1085.
- [5] M.H. Ramlee, M.R. Abdul Kadir, M.R. Murali, T. Kamarul, Finite element analysis of three commonly used external fixation devices for treating Type III pilon fractures, *Med. Eng. Phys.* 36 (10) (2014) 1322–1330.
- [6] L. Yao, W. Zhang, G. Yang, Y. Zhu, Q.L. Zhai, C.F. Luo, Morphologic characteristics of the posterior malleolus fragment: a 3-D computer tomography based study, *Arch. Orthop. Trauma Surg.* 134 (3) (2014) 389–394.
- [7] R.A. Agha, M.R. Borrelli, M. Vella-Baldacchino, R. Thavayogan, D.P. Orgill, for the STROCSS Group, The STROCSS statement: strengthening the reporting of cohort studies in surgery, *Int. J. Surg.* 46 (2017) 198–202.
- [8] F.A. Bandak, R.E. Tannous, T. Toridis, On the development of an osseo-ligamentous finite element model of the human ankle joint, *Int. J. Solids Struct.* 38 (10) (2001) 1681–1697.
- [9] Z.J. Zhu, Y. Zhu, J.F. Liu, Y.P. Wang, G. Chen, X.Y. Xu, Posterolateral ankle ligament injuries affect ankle stability: a finite element study, *BMC Musculoskelet. Disord.* 17 (1) (2016) 96.
- [10] D.D. Anderson, J.K. Goldsworthy, W. Li, M. James-Rudert, Y. Tochigi, T.D. Brown, Physical validation of a patient-specific contact finite element model of the ankle, *J. Biomech.* 40 (8) (2007) 1662–1669.
- [11] C. Hurschler, J. Emmerich, Nikolaus Wülker, In vitro simulation of stance phase gait part I: model verification, *Foot Ankle Int./American Orthopaedic Foot and Ankle Society [and] Swiss Foot and Ankle Society* 24 (8) (2003) 614–622.
- [12] D.T. Meijer, J.N. Doornberg, I.N. Sierevelt, et al., Guesstimation of posterior malleolar fractures on lateral plain radiographs, *Injury-international Journal of the Care of the Injured* 46 (10) (2015) 2024–2029.
- [13] H.M. Zhao, X.J. Liang, Y. Li, G.R. Yu, Y.F. Yang, D.S. Zhang, Effect of various reduction degrees of posterior malleolus fracture on tibiotalar joint contact, *Chin. J. Traumatol.* 30 (10) (2014) 1035–1039 (in Chinese).